Carnegie Observatories Astrophysics Series, Vol. 4:
Origin and Evolution of the Elements, 2004
ed. A. McWilliam and M. Rauch (Pasadena: Carnegie Observatories,
http://www.ociw.edu/ociw/symposia/series/symposium4/proceedings.html)

Histories of the Milky Way Dwarf Spheroidal Galaxies and ω Centauri

T. TSUJIMOTO[1] and T. SHIGEYAMA[2]
(1) National Astronomical Observatory, Tokyo, Japan
(2) University of Tokyo, Tokyo, Japan

Abstract

We describe the star formation histories of the Milky Way dwarf spheroidal galaxy and a globular cluster ω Centauri in terms of an inhomogeneous chemical evolution model developed for the halo of the Milky Way. The observed abundance trends seen in neutron-capture elements together with α-elements constrain our models to shed light on the histories of these nearby galaxies and ω Cen. A new picture of the globular cluster formation scenario induced by cloud-cloud collisions is also presented.

1.1 Introduction

There is no room for doubt that the recent progress on abundance determination for numerous solar neighborhood stars promotes a better understanding of the nature of the Milky Way because stellar abundance patterns bring us valuable information on how the Milky Way formed and has evolved (Wheeler, Sneden, & Truran 1989; McWilliam 1997). In this section, we present a new chemical evolution model for the Galactic halo as well as an interpretation of the abundance features seen in the Galactic halo field stars.

In the usual approach (Tinsley 1980), stars are assumed to form from well-mixed gas at a rate proportional to some power of the gas density (Schmidt 1959). However, the validity of using this assumption for halo stars has been challenged by the observed abundance patterns of very metal-poor stars (McWilliam et al. 1995; Ryan, Norris, & Beers 1996), which are incompatible with those predicted from such a simple star formation rate. This problem has recently been overcome by a newly proposed model in which halo stars are always born from dense shells swept up by individual supernova remnants (SNRs) and necessarily retain the abundance patterns of heavy elements ejected from supernovae (SNe) of various progenitor masses (Shigeyama & Tsujimoto 1998; Tsujimoto & Shigeyama 1998; Tsujimoto, Shigeyama, & Yoshii 1999, 2000).

This model was motivated by the fact that the mixing length of heavy elements ejected from SNe is too small to achieve chemical homogeneity over the entire halo. Current estimates of velocity dispersion and total mass of the stellar components in the Galactic halo indicate that consecutive star-forming processes are likely to have been confined in separate regions or clouds having mass scales of $M_c \approx 10^{6-7} M_\odot$, which make up the entire baryonic halo. In a proto-galaxy, the metal-free Population III stars of the first generation could have been born in highly compressed layers behind shock waves caused by supersonic initial turbulence. The massive ones of them eventually explode as metal-free SNe, which trigger the

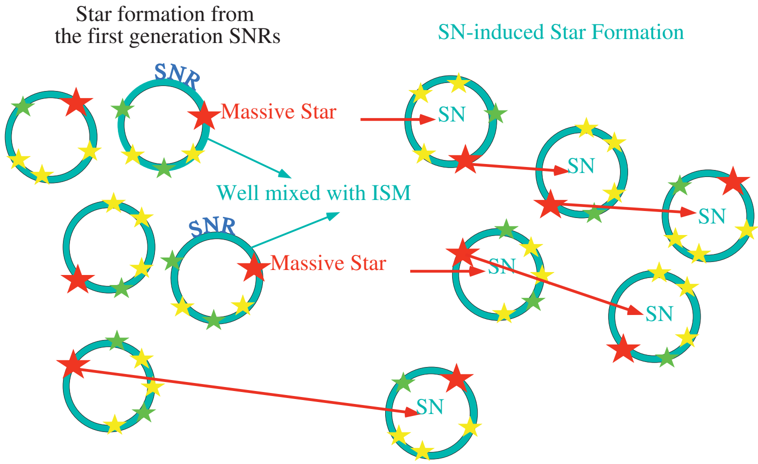

Fig. 1.1. Schematic illustration of the SN-induced star formation.

formation of stars in dense shells of mass M_{sh}. The mass M_{sh} is approximated by the formula (Shigeyama & Tsujimoto 1998)

$$M_{sh} = 6.5 \times M_{\odot} \left(\frac{E_0}{10^{51}\ \mathrm{ergs}} \right)^{0.97} \times n_1^{-0.062} \left(\frac{\sigma_v}{10\ \mathrm{kms}^{-1}} \right)^{-9/7} , \tag{1.1}$$

where E_0: the explosion energy of an SN, n_1: the density of an interstellar medium (ISM), and σ_v: the velocity dispersion of the ISM. This SN-induced formation of stars goes into generations, as schematically illustrated in Fig. 1.1, and terminates when SNRs become unable to sweep up enough gas to form dense shells.

In this picture, the abundance pattern of each star is composed not only of the heavy elements ejected from an SN of the preceding generation but also of those that have been already included in the ISM swept up by the SNR. However, very metal-poor halo stars might have inherited the abundance pattern for the ejecta of the preceding SN due to a negligible contribution from heavy elements in the ISM to their stellar abundances. From this viewpoint, a unique feature in the observed distribution of [Ba/Mg] *vs.* [Mg/H] for very metal-poor stars can be adequately interpreted as shown in Fig. 1.2. We associate this feature, a bifurcation of the observed elemental ratios into two branches in the Mg abundance interval $-3.7 \leq [\mathrm{Mg/H}] \leq -2.3$, with two distinct processes. The first branch, which we call the "y"-branch, is associated with the production of Ba and Mg from individual massive SNe. We conclude that SNe II with $M_{\rm ms} \approx 20 M_{\odot}$ are the dominant source of r-process nucleosynthesis in the early Galaxy. An SN-induced chemical evolution model with the $M_{\rm ms}$-dependent Ba yield creates the y-branch, reflecting the different nucleosynthesis yields of [Ba/Mg] for each SN II with $M_{\rm ms} \gtrsim 20 M_{\odot}$. The second branch, which we call the "i"-branch, is associated with the elemental abundance ratios of stars which were formed in the dense shells of the ISM swept up by SNe II with $M_{\rm ms} < 20 M_{\odot}$ that do *not* synthesize r-process elements, and applies to stars with observed Mg abundances in the range [Mg/H]$<$ -2.7. The Ba abundances in these stars reflect those of the interstellar gas at the (later) time of their formation. The existence of a [Ba/Mg] i-branch strongly suggests that SNe II

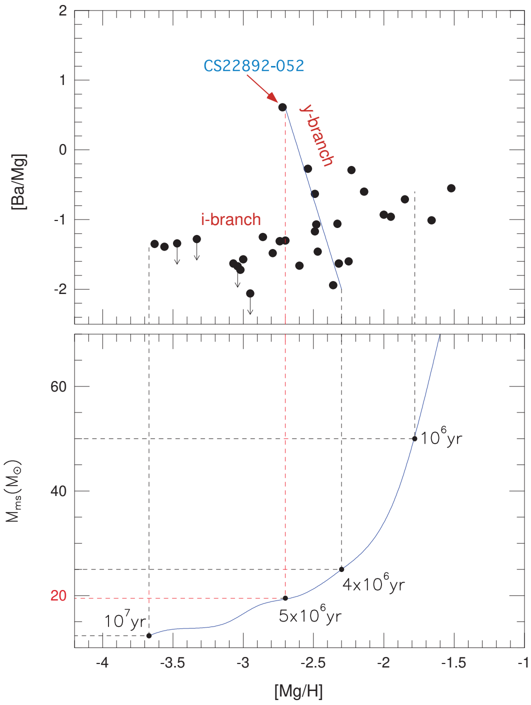

Fig. 1.2. *upper panel:* the correlation of [Ba/Mg] with [Mg/H] for metal-poor stars (McWilliam 1998). The thick line is the left-side boundary to the *y*-branch representing the mass range of the *r*-process site. *lower panel:* SN II progenitor mass $M_{\rm ms}$ plotted as a function of [Mg/H] inside the shell swept up by the SNR. The stellar lifetimes are also shown for four reference masses of $M_{\rm ms}$ = 12, 20, 25, and $50M_\odot$. Dashed lines in the lower and upper panels illustrate how we assign $M_{\rm ms}$ to each star along the boundary.

which are associated with stars of progenitor mass $M_{\rm ms} \leq 20M_\odot$ are infertile sources for the production of *r*-process elements.

These findings together with the recent progress on abundance determination beyond the solar neighborhood lead us to carry our study forward to the chemical evolution for the Milky Way dwarf spheroidal (dSph) galaxies and the peculiar globular cluster ω Centauri.

1.2 The Milky Way Dwarf Spheroidal Galaxies

We have now reached the stage where we can learn the history of other nearby galaxies from detailed elemental abundances of individual stars. Remarkable features in the abundance patterns of dSph stars are found in neutron-capture elements such as Ba and Eu, and also in α-elements. Using these elemental abundance features, we discuss the history and star formation of dSph galaxies.

1.2.1 History of dSph galaxies

Stellar abundance pattern of *n*-capture elements is used as a powerful tool to infer how the star formation proceeded in dSph galaxies. It is found that the abundance correlation of Ba with Fe in stars belonging to dSph galaxies orbiting the Milky Way, i.e.,

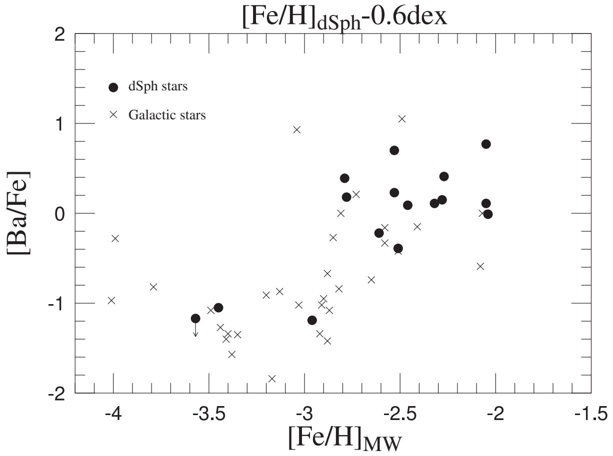

Fig. 1.3. Correlations of [Ba/Fe] with [Fe/H] for dSph stars (filled circles; Shetrone et al. 2001) and Galactic halo field stars (McWilliam 1998). The data of dSph stars are shifted by the amount of Δ[Fe/H]=–0.6 dex (see the text). The K star of Ursa Minor is excluded from the plots because it is recognized to be a carbon star, most probably self-enriched by *s*-process material.

Draco, Sextans, and Ursa Minor have a feature similar to that in Galactic metal-poor stars. Fig. 1.3 shows the correlation of [Ba/Fe] with [Fe/H] for dSph stars (Shetrone et al. 2001), together with that for Galactic metal-poor stars (*crosses*; McWilliam 1998). Filled circles represent dSph stars with [Fe/H] shifted by Δ[Fe/H] = –0.6 dex. An excellent coincidence between two distributions appears: both metal-poor stars and dSph stars populate two separate branches in the [Ba/Fe]-[Fe/H] plane, i.e., the first *y*-branch in which stars have positive [Ba/Fe] ratios (i.e., greater than the solar ratio), and the second *i*-branch with the upper bound at [Ba/Fe]=–1. This feature can be reproduced by our inhomogeneous chemical evolution model as already described in the previous section.

The metallicities of metal-poor stars are determined by two factors: how much mass of heavy elements a SN supplies and how much mass of ISM was eventually swept by a single SN explosion (Shigeyama & Tsujimoto 1998). The former is determined exclusively by each SN. On the other hand, the latter quantity is influenced by the environment such as the velocity dispersion σ_v and density n_1 of the ISM. If SNe in the Milky Way and those in dSph galaxies are similar, different environments should give rise to the Δ [Fe/H] discussed above. Since the mass M_{sh} swept up by an SN is much more sensitive to the velocity dispersion than to the density; $M_{sh} \propto \sigma_v^{-9/7} n_1^{-0.062}$ (see equation (1.1)), it is likely that a larger velocity dispersion in dSph galaxies at the star formation epoch enhanced the stellar [Fe/H]. Quantitatively, Δ [Fe/H]=–0.6 dex corresponds to a velocity dispersion of $\sigma_v \sim 26$ km s^{-1}. The velocity dispersion $\sigma_\star$ of stars must have a similar value in equilibrium configuration. The present value of $\sigma_\star$ measured in Galactic dSph galaxies are about 9 km s^{-1}. These two significantly different velocity dispersions can be connected in the context of a galaxy losing mass by the tidal force of the Milky Way. As a result, the total mass of each dSph galaxy is found to have been originally $\sim$ 25 times larger than at present, using the relation $\sigma_\star \propto M_{\rm dSph}^{1/3}$.

Then the history of Galactic dSph galaxies that we have proposed is as follows. The proto-dSph galaxy consisted of gas and dark matter, and was approximately 25 times as massive as a present dSph galaxy. Star formation lasted for about two hundred million years; meanwhile, $\sim$ 5 percent of the gas converted into stars, which has been estimated from the chemical evolution model for dSph galaxies (Tsujimoto & Shigeyama 2002). Afterward, the remaining gas was dispelled by the last SN explosions. On the other hand, dark matter which surrounds stars has lost more than 90% of its mass through the tidal interaction with the Milky Way.

1.2.2 Why the Low [α-elements/Fe] Ratios in dSph Galaxies?

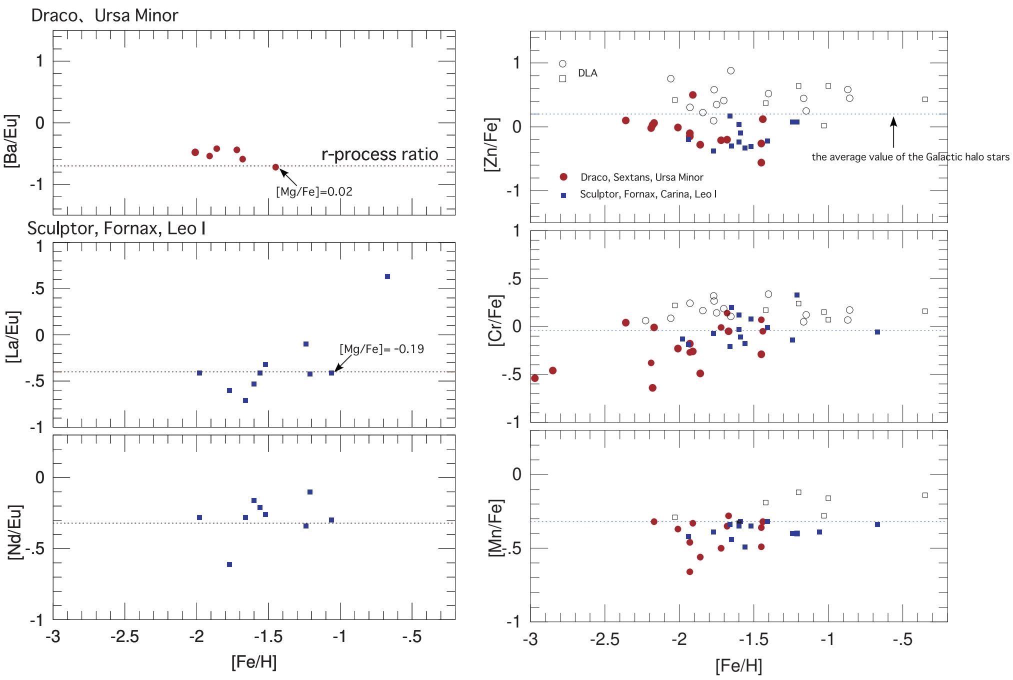

Fig.1.4.*left panel:* the *s*- and *r*-process elemental ratios for dSph stars. Red circles show the [Ba/Eu] ratios for Draco and Ursa Minor (Shetrone et al. 2001), and blue squares denote the [La, Nd/Eu] ratios for Sculptor, Fornax, and Leo I (Shetrone et al. 2003). The dashed lines represent the pure *r*-process abundance ratios. For reference, the [Mg/Fe] ratios for two stars which exactly show the pure *r*-process ratios are attached. *right panel:* the ratios of Fe-peak elements to Fe for dSph stars (*red circles* and *blue squares*) together with those for DLA (*open circles*; Prochaska & Wolfe 2002, *open squares*; Pettini et al. 2000). The dashed lines represent the average [X/Fe] ratios of the Galactic halo stars.

A puzzling abundance feature has been seen in the [α-elements/Fe] ratios for dSph stars. Shetrone et al. (2001, 2003) found that dSph stars exhibit lower [α-elements/Fe] ratios than stars in the Galactic halo. A likely interpretation of these observational results is that dSph

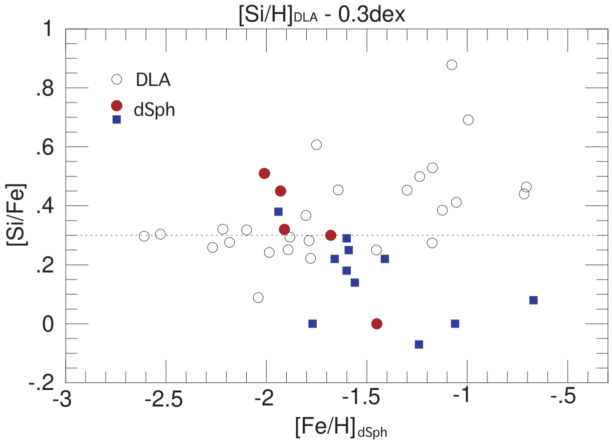

Fig. 1.5. Correlations of [Si/Fe] with [Fe/H] for dSph stars (Shetrone et al. 2001, 2003) and [Si/H] for DLA (Prochaska & Wolfe 2002). Data of DLA are shifted by Δ[Si/H]=-0.3 dex. The dashed line shows the average [Si/Fe] ratio of the Galactic halo stars.

galaxies experienced different enrichment by SNe from the Galactic halo (e.g., Shetrone et al. 2003). It has two possibilities. One is a contribution from SNe Ia in dSph galaxies. However, as shown on the left panel of Fig. 1.4, abundance ratios among n-capture elements for most of dSph stars exhibit nearly pure r-process ratios. For Sculptor, Fornax, and Leo I, we show the [La, Nd/Eu] ratios instead of [Ba/Eu] because the La/Eu ratio could be better s-/r-process indicator than the Ba/Eu ratio due to large uncertainties involved in abundance determination of Ba/Eu ratios (Sneden, Cowan, & Truran 2001). Taking into account a longer lifetime of SN Ia progenitors than s-process enrichment, the idea that a large amount of Fe from SNe Ia lowered the [α-elements/Fe] ratios is unlikely. Thus the proposal by Shetrone et al. (2003) that the plateau-like [Cu, Mn/Fe] ratios seen in dSph stars can be explained by the metallicity-dependent production of these elements in SNe Ia (i.e., little production of Cu and Mn at the explosions of low-metallicity SNe Ia) seems problematic in this regard. Another possibility is different yields from SNe II, likely due to a different initial mass function (IMF) in dSph galaxies from a Salpeter's. However, there is no signature for other elemental ratios such as [Mn/Fe]. It is therefore also unlikely.

Here we will deliberate on this problem from a different angle. As shown on the right panel of Fig. 1.4, abundance ratios for dSph stars are distributed over the opposite side of DLA's with average values for Galactic halo stars in the middle. If we interpret abundance trends of DLA as a result of dust depletion, abundance patterns for dSph stars might turn out to reflect those for dust grain, which implies that dSph stars were born from dust-dominated materials (or accretion of dust grain onto the surface of dSph stars ?). If this is the case, low [α-elements/Fe] ratios can be naturally explained for Mg and Si (see Fig. 1.5), though some doubts on the cases for Ca and Ti remain. Here we plot the [Si/Fe] ratios for DLA against [Si/H] because the [Si/Fe] trend with respect to [Si/H] is more clear than against [Fe/H] as already shown by Prochaska & Wolfe (2002). It should be noted that such an idea is questionable at least from the argument that dust-to-gas ratio in dSph galaxies is expected to be much smaller than $\sim$0.02 due to a low-metal content (e.g., Whittet 1992). In any case, abundance features relevant to relation between dSph stars and DLA might help us solve the puzzling problem "low [α-elements/Fe] ratios in dSph galaxies".

1.3 ω Centauri

The potential history and characteristics of the globular cluster (GC) ω Centauri remains largely unresolved, although its most conspicuous features can be seen in the elemental abundance properties. Most prominently, there exists a large dispersion in metallicity (–2 $\lesssim$ [Fe/H] $\lesssim$ –0.5) among its member stars (e.g., Norris & Sa Costa 1995; Suntzeff & Kraft 1996) in contrast to other Galactic GCs which exhibit essentially no dispersion. In addition, this GC contains stars that display a significant enhancement of *s*-process elements relative to Fe and *r*-process elements (Norris & Da Costa 1995).

Regarding the latter feature, a study by Smith et al. (2000) identified two distinct populations in terms of correlation between [Ba/Eu] and [Fe/H] for 10 ω Cen stars (*filled circles* in Fig. 1.6). One population has metallicity in the range of [Fe/H]< -1.8 and low [Ba/Eu] ratios, corresponding closely to the pure *r*-process origin ratio, and the other population has [Fe/H]> -1.6 with high [Ba/Eu] ratios, ascribed to a large *s*-process nucleosynthesis contribution. Another unique feature of the elemental abundance can be observed in the abundance distribution function (ADF) of ω Cen stars (Norris, Freeman, & Mighell 1996; Suntzeff & Kraft 1996; van Leeuwen et al. 2000). The ADF has a conspicuous peak at [Fe/H]~ -1.4 with a long, metal-rich tail starting from [Fe/H]~ -1 extending to [Fe/H]$\sim$ –0.5. It is expected that both the unusual ADF and the peculiar behavior of *n*-capture elements could be useful in inferring the potentially unique history of ω Cen.

1.3.1 Star Formation History of ω Cen

The star formation history of ω Cen is inferred from the stellar elemental abundance pattern shown in Fig. 1.6. First of all, a sudden increase in the [Ba/Eu] ratios at [Fe/H]~ -1.6 implies that ω Cen has undergone two discrete episodes of star formation. The observed [Ba/Eu] ratios of as large as +1 are attributed to a contribution from asymptotic giant branch (AGB) stars after gas removal at the end of the first episode of star formation. If gas was not expelled after the first episode, the *s*-process nucleosynthesis in AGB stars would increase the [Ba/Eu] ratio to only $\sim$ +0.2 at most according to the Salpeter IMF.

The star formation history inferred from the observed [Ba/Eu] ratios is then as follows. 1. After completion of the first phase of star formation, a large part of the remaining gas was expelled by SN II explosions. 2. The gas was then contaminated by *s*-process elements ejected from AGB stars during a quiescent stage lasting several hundred Myr. This led to the enhancement of Ba relative to Eu in the gas. 3. Star formation then recommenced after the gas, once heated by SNe, cooled sufficiently and collapsed, with associated shock wave formation. Stars formed from this shocked gas and stars subsequently formed have very high Ba/Eu ratios. The second star formation phase continued until the metallicity [Fe/H] reached ~ -1.

This then poses the question of how star formation proceeded after the second star formation epoch. A clue lies in the extended metal-rich tail in the observed ADF. Pancino et al. (2002) recently found that stars belonging to the metal-rich tail exhibit decreasing [Ca/Fe] ratios with increasing [Fe/H], ascribed as a sign of SNe Ia enrichment (*open circles* in Fig.1.6). From the theoretical aspect, such SNe Ia enrichment is indispensable to increasing the metallicity [Fe/H] of stars to $\sim$ –0.5 as observed. In fact, this metal rich end of

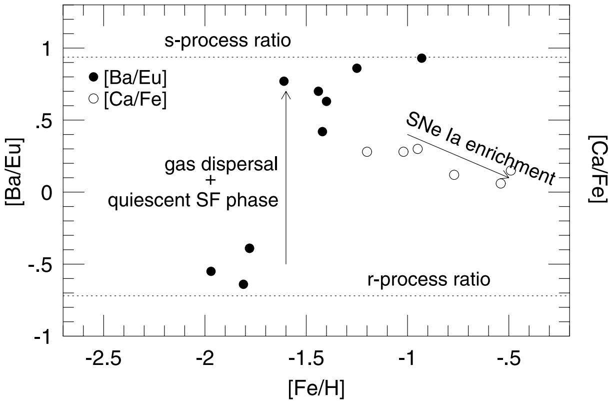

Fig. 1.6. Correlations of [Ba/Eu] (*filled circles*; Smith et al. 2000) and [Ca/Fe] (*open circles*; Pancino et al. 2002) with [Fe/H] for ω Cen stars. The dashed lines show the [Ba/Eu] ratios theoretically anticipated from the *r*-process origin and *s*-process nucleosynthesis. Some comments are also attached.

[Fe/H] cannot be reached by the Fe supply from only SNe II given the small number of stars with [Fe/H] > -1. In the SN-induced star formation scenario, SNe Ia do not only enrich gas with Fe but also initiate star formation in the third episode. In the end, ω Cen has three episodes of star formation, each of which is likely to be identified with each subpopulation found by Pancino et al. (2000).

1.3.2 Globular Cluster Formation Scenario

The uniqueness of ω Cen has led some authors to consider that it is the surviving nucleus of a dwarf galaxy that has been tidally stripped by the Milky Way (e.g., Freeman 1993). It should be noted that there are no observed metal-poor ([Fe/H] $\lesssim$ –2) stars in ω Cen, which indicates that ω Cen formed from a pre-enriched gas. This feature is indeed shared with the other GCs. The formation of ω Cen should therefore be considered in any general scheme of GC formation. Here we propose that GCs formed through collisions of the proto-cluster clouds at the halfway of SN-induced star formation. Cloud-cloud collisions can leave shocked gas with some heavy elements but without stars or dark matter.

After two clouds collide, strong shock waves are formed, which compress the gas and leave a dense cloud with sufficient mass for star formation if the collision is nearly head-on. From this compressed gas, stars are assumed to form with metallicity inherited from the gas. In the SN-driven star formation scenario, the star formation history is determined by the evolution of SNRs, which is affected by the environment. A critical indicator of chemical evolution is whether star formation proceeded for a number of generations or ceased after only one or a few generations. This condition is given by comparing the maximum size that an SNR can attain and the size of the cloud. If the maximum size of an SNR exceeds the size of the cloud, the SNR cannot assemble the gas necessary to form stars of the next generation. The resultant GC would then contain a single generation of stars with no dispersion in [Fe/H]. If the SNR is smaller than the cloud, the cloud would contain multiple generations of stars with different [Fe/H], resembling ω Cen stars. This criterion gives the maximum velocity that can produce a GC with some dispersion in [Fe/H], as follows,

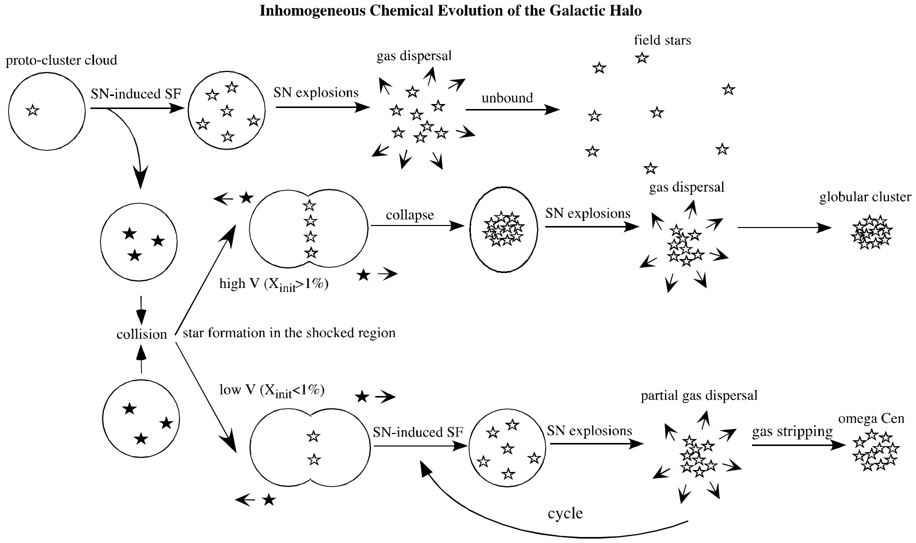

Fig. 1.7. Schematic picture of inhomogeneous chemical evolution model for the Galactic halo.

$$v_{1,\max} \sim 33\,\mathrm{km\ s^{-1}}\left(\sigma_v/10\,\mathrm{km\,s^{-1}}\right)^{37/28}\left(M/10^6 M_\odot\right)^{1/4}. \qquad (1.2)$$

Since clouds move at ~ 200 km s^{-1} in the gravitational potential of the Milky Way, it is rare that two clouds would collide with such low velocity as long as each cloud has a mass of $\sim 10^6 M_\odot$ corresponding to the Jeans mass soon after recombination.

An additional condition for the formation of multiple generations of stars is that the mass fraction $X_{\rm init}$ of stars in a cloud at the beginning should be less than 1%, as discussed previously Tsujimoto et al. (1999). If $X_{\rm init}$ is larger than 1%, the total gas swept up by the first SNRs exceeds the entire amount of available gas, and thus star formation stops at the first or with a few generations.

The mass and velocity dispersion of the proto-cluster cloud generating ω Cen have been estimated to be $M \sim 3 \times 10^7 M_\odot$, $\sigma_v \sim 36$ km s^{-1} from the chemical evolution model (Tsujimoto & Shigeyama 2003). These values together with equation (1.2) suggest that a supernova does not break up the shocked clouds if two proto-cluster clouds collide with relative velocity ($2v_1$) of less than ~ 700 km s^{-1}. Therefore, ω Cen-like clusters are most likely to form from two colliding massive clouds if $X_{\rm init}$ is less than 1%. Such a small $X_{\rm init}$ could be realized by a small relative velocity leading to weak shock-wave compression. After a small mass fraction ($X_{\rm init} < 1\%$) of first-generation stars had formed in colliding proto-cluster clouds, chemical enrichment due to SN-induced star formation would then have proceeded in ω Cen. The scheme of GC formation discussed here is described in Fig. 1.7.

1.4 Conclusions

Here we show that stellar elemental abundance patterns for n-capture elements give us a deep insight into the star formation histories for nearby galaxies and ω Cen. Our finding is brought by two characteristics of n-capture elements; (i) the correlation of [r-process/Fe] with [Fe/H] in stellar abundances has a quite unique feature as seen in the Galactic halo stars, and (ii) two distinct types of *n*-capture processes, i.e., *r*- and *s*-processes, occur in a different site, which yields the time difference in the contribution to the enrichment in the ISM between two processes. In addition, the [α-elements/Fe] ratio which should represent the SN II/SN Ia ratio and thus serve as a nucleosynthesis clock as well as the *s*-/*r*-process elemental ratio is another powerful tool to infer the star formation history, though this might not be the case for dSph galaxies.

References

Freeman, K. C. 1993, in ASP Conf. Ser. 48, The Globular Cluster-Galaxy Connection, ed. G. H. Smith & J. P. Brodie (San Francisco: ASP), 608
McWilliam, A., Preston, G. W., Sneden, C., & Searle, L. 1995, AJ, 109, 2757
McWilliam, A. 1997, ARA&A, 35, 503
McWilliam, A. 1998, AJ, 115, 1640
Norris, J. E., & Da Costa, G. S. 1995, ApJ, 447, 680
Norris, J. E., Freeman, K. C., & Mighell, K. J. 1996, ApJ, 462, 241
Pancino, E., Ferraro, F. R., Bellazzini, M., Piotto, G., & Zoccali, M. 2000, ApJ, 534, L83
Pancino, E., Pasquini, L., Hill, V., Ferraro, F. R., & Bellazzini, M. 2002, ApJ, 568, L101
Pettini, M., Ellison, S. L., Steidel, C. C., Shapley, A. E., & Bowen, D. V. 2000, ApJ, 532, 65
Prochaska, J. X., & Wolfe, A. M. 2002, ApJ, 566, 68
Ryan, S. G., Norris, J. E., & Beers, T. C. 1996, ApJ, 471, 254
Schmidt, M. 1959, ApJ, 129, 243
Shetrone, M. D., Côté, P., & Sargent, W. L. 2001, ApJ, 548, 592
Shetrone, M. D., Venn, K. A., Tolstoy, E., Primas, F., Hill, V., & Kaufer, A. 2003, AJ, 125, 684
Shigeyama, T., & Tsujimoto, T. 1998, ApJ, 507, L135
Smith, V. V., Suntzeff, N. B., Cunha, K., Gallino, R., Busso, M., Lambert, D. L., & Straniero, O. 2000, AJ, 119, 1239
Sneden, C., Cowan, J. J., & Truran, J. W. 2001, in Cosmic Evolution, ed. E. Vangioni-Flam, R. Ferlet, & M. Lemoine (New Jersey: World Scientific), 179
Suntzeff, N. B., & Kraft, R. P. 1996, AJ, 111, 1913
Tinsley, B. M. 1980, Fund. Cosmic Phys., 5, 287
Tsujimoto, T., & Shigeyama, T. 1998, ApJ, 508, L151
Tsujimoto, T., Shigeyama, T., & Yoshii, Y. 1999, ApJ, 519, L63
Tsujimoto, T., Shigeyama, T., & Yoshii, Y. 2000, ApJ, 531, L3
Tsujimoto, T., & Shigeyama, T. 2002, ApJ, 571, L93
Tsujimoto, T., & Shigeyama, T. 2003, ApJ, 590, 803
Wheeler, J. C., Sneden, C., & Truran, J. W. 1989, ARA&A, 27, 279
Whittet, D. C. B. 1992, Dust in the Galactic Environment (Bristol: Institute of Physics Publishing)